

JAAS

Journal of Analytical Atomic Spectrometry

Accepted Manuscript

This article can be cited before page numbers have been issued, to do this please use: R. Sánchez, F. Chainet, V. Souchon, S. Carbonneaux, C. P. Lienemann and J. Todoli Torro, *J. Anal. At. Spectrom.*, 2020, DOI: 10.1039/D0JA00156B.



This is an Accepted Manuscript, which has been through the Royal Society of Chemistry peer review process and has been accepted for publication.

Accepted Manuscripts are published online shortly after acceptance, before technical editing, formatting and proof reading. Using this free service, authors can make their results available to the community, in citable form, before we publish the edited article. We will replace this Accepted Manuscript with the edited and formatted Advance Article as soon as it is available.

You can find more information about Accepted Manuscripts in the [Information for Authors](#).

Please note that technical editing may introduce minor changes to the text and/or graphics, which may alter content. The journal's standard [Terms & Conditions](#) and the [Ethical guidelines](#) still apply. In no event shall the Royal Society of Chemistry be held responsible for any errors or omissions in this Accepted Manuscript or any consequences arising from the use of any information it contains.

Journal Name

ARTICLE

SILICON SPECIATION IN LIGHT PETROLEUM PRODUCTS USING GAS CHROMATOGRAPHY COUPLED TO ICP-MS/MS

Raquel Sánchez,^{a,*} Fabien Chainet,^{b,*} Vincent Souchon,^b Sylvain Carbonneau,^b Charles-Philippe Lienemann,^b José-Luis Todolí^a

Received 00th January 20xx,
Accepted 00th January 20xx

DOI: 10.1039/x0xx00000x

Silicon speciation in light petroleum products through the hyphenation of gas chromatography coupled to ICP–tandem mass spectrometry (GC-ICP-MS/MS) is described in the present work. Eleven silicon compounds (nine siloxanes, trimethylsilanol and triethylsilane) have been taken as model molecules. The carrier and optional gas flow rates as well as the hydrogen gas flow rate in the octopole reaction cell (ORC) were critical variables. They precluded both the sensitivity and the extent of the effects caused by the sample matrix and silicon nature. The optimization of the latter variable mitigated the m/z 28 interference ($^{14}\text{N}^{14}\text{N}^+$ and $^{12}\text{C}^{16}\text{O}^+$). Moreover, under the optimized conditions, a universal response was found irrespectively of the silicon chemical form and sample matrix. The analytical performances of the method have been evaluated. Thus, the ICP-MS/MS response was linear between 0 to 500 $\mu\text{g kg}^{-1}$ with correlation coefficients up to 0.999, whereas the limit of quantification (LOQ) ranged from 8 to 60 $\mu\text{g kg}^{-1}$. Moreover, no drift was found for quality control samples analysed along a given analytical run. Only, the most volatile compound, *i.e.*, trimethylsilanol (TMSOH), induced a drop in sensitivity caused by its partial evaporation from the GC vial. The method was validated by the analysis of real samples and the results were compared with those obtained by inductively coupled plasma optical emission spectrometry (ICP-OES) and X-rays fluorescence. No significant differences in Si total content provided by the three methods were found. These results demonstrated that all silicon species were taken into account using the GC-ICP-MS/MS as speciation method. Real light petroleum products, especially coker naphtha samples, were analyzed and it was verified that they only contained cyclic siloxanes (D3–D6), mainly hexamethylcyclotrisiloxane (D3) and octamethylcyclotetrasiloxane (D4).

1 Introduction

Silicon plays a crucial role in many fields such as food analysis, semiconductor and steel industry.¹ Especially relevant is its study in the petroleum industry due to its poisoning effect on hydrogenation catalysts during the refining process.^{2,3} In fact, silicon species adsorbed at the surface of the catalyst, thus decreasing its activity with a great economic impact. Interestingly, the extent of this effect depends on the chemical structure of silicon compounds.^{4–7} The main source of silicon compounds is the polydimethylsiloxane (PDMS) thermal degradation. This compound is usually injected to enhance oil recovery (EOR) or used as an antifoaming agent during refining processes.^{8,9} Among the different silicon compounds, cyclic siloxanes have been identified as the major PDMS degradation

products with some traces of linear polysiloxanes.¹⁰ Therefore, silicon speciation must be achieved in order to fully characterize this element in hydrotreatment feeds.¹

In petroleum products total silicon concentration is at the trace level, ranging from hundreds of $\mu\text{g kg}^{-1}$ to several mg kg^{-1} .^{1,11} Therefore sensitive and accurate methods are needed to quantify this element. The most common techniques for carrying out this kind of determinations are inductively coupled plasma optical emission spectrometry (ICP-OES)^{12,13} and mass spectrometry (ICP-MS).¹⁴ However, this situation becomes more complex when speciation analysis is required. Note that a gasoline sample may contain around 200 different hydrocarbon compounds.¹¹

Several powerful analytical tools, such as normal phase high-performance liquid chromatography–mass spectrometry (HPLC-ICP-MS),¹⁴ size-exclusion ICP-MS,¹⁴ gas chromatography–mass spectrometry (GC-MS) in the single ion monitoring (SIM) mode,¹¹ Fourier transform ion cyclotron resonance mass spectrometry (FT-ICR/MS),¹⁵ heart-cutting gas chromatography coupled to time of flight mass spectrometry (GC-GC-TOF/MS)¹⁶ and GC-ICP-MS¹⁷ have been developed using model molecules in solvents and spiked gasolines for silicon speciation. Taking into account the limitations

^a Department of Analytical Chemistry, Nutrition and Food Science
University of Alicante
P.O. Box 99, 03080, Alicante, Spain

^b IFP Energies Nouvelles
Rond-point de l'échangeur de Solaize, BP 3, F-69360 Solaize, France
e-mail: fabien.chainet@ifpen.fr
Electronic Supplementary Information (ESI) available: [details of any supplementary information available should be included here]. See DOI: 10.1039/x0xx00000x

presented by each one of the individual techniques, Chainet *et al.*^{16,18} proposed an analytical strategy based on several techniques in order to identify the silicon species coming from synthetic PDMS degradation samples, in particular those compounds responsible for downstream catalyst poisoning in real samples.

Hyphenation of GC with a sensitive and specific detection such as inductively coupled plasma mass spectrometry (ICP-MS) could be considered as a powerful tool for Si speciation in petroleum products.^{1,17} However, this is not an easy task, due to the spectral interferences found at the ²⁸Si major isotope caused by ¹²C¹⁶O⁺ and ¹⁴N¹⁴N⁺ in a lesser extent.^{17,19} The presence of carbon, together with the addition of oxygen to avoid the clogging of the ICP-MS sampling cone, causes the formation of ¹²C¹⁶O⁺ and degrades the sensitivity of the technique due to high background signal.^{17,20} In order to overcome these spectral interferences, ICP high resolution mass spectrometry (HRMS) coupled with micro-size exclusion chromatography (μ -SEC) has been employed.^{18,21} However, the limit of quantification was on the order of 1 mg kg⁻¹. In a different approach, ICP high resolution mass spectrometry (HRMS) has been coupled to normal phase-HPLC for the speciation of standard silicon compounds in xylene.¹⁴ Two drawbacks were found: first, it was observed that not all the silicon compounds eluted from the column; and, second the method could not be applied for silicon speciation in petroleum products under the proposed chromatographic conditions.

The use of an ICP-MS equipped with a dynamic reaction cell (DRC) has been proposed as a powerful tool to resolve polyatomic interferences on ²⁸Si.^{22,23} NH₃ has been used as reactant gas to determine silicon traces in steels.²⁴ The presence of this reduced the background noise signal. However, reaction between Si⁺ and NH₃ yielding SiNH₂⁺ (m/z 44), considerably lowers the signal on ²⁸Si.²⁵ Oxygen was demonstrated as an effective alternative to overcome spectral interferences at m/z 28 by the formation of ²⁸Si¹⁶O⁺.²⁶ Hydrogen has been used as an alternative reactant gas. Chainet *et al.*¹⁷ In this case, silicon did not react with hydrogen whereas ¹⁴N¹⁴N⁺ and ¹²C¹⁶O⁺ did, what decreased the spectral background noise. Although Si profiles have been obtained in acetone as solvent, the matrix effect was not studied and a non-universal response for Si compounds was observed. Very recently Foppiano *et al.*²⁷ proposed a mixture of He and H₂ as reactant gas for the determination of siloxane compounds in biogas samples.

In 2012, the introduction of a new type of quadrupole-based ICP/MS device, the so-called ICP-tandem mass spectrometer (ICP-MS/MS) allowed the improvement of the spectral interferences resolution by offering superior control in the cell chemistry.²⁸ The capabilities of the ICP-MS/MS were recently demonstrated for complex organic matrices for solving interferences and reducing detection limits.²⁹ Nelson *et al.*³⁰ applied GC-ICP-MS/MS for S, Cl and P detection in foods. More recently, a GC-ICP-MS/MS instrumental setup was successfully developed for the determination of the content of sulfur and its species in gasoline.³¹ In 2020, Radermacher *et al.*³² proposed the GC-ICP-MS/MS coupled for cyclic volatile methylsiloxanes determination in fish samples after a solid-liquid extraction procedure. However, to our knowledge, the potential of GC-ICP-MS/MS for the direct speciation of a difficult element like Si in complex matrices without previous extraction method has not been reported yet in the

literature. The aim of the present work was thus to develop a GC-ICP-MS/MS method for silicon speciation in light petroleum products. First GC-ICP-MS/MS optimization was carried out using hydrogen as reactant gas. It allowed successful detection of silicon with a complete resolution of interferences. One of the main goals of the present work was to develop a method in which the influence of the matrix nature and the silicon chemical form on sensitivity was minimized. Once the analytical figures of merit were evaluated, the method was validated and applied to the analysis of real light petroleum products.

Experimental

Standard solutions and samples

Silicon standards. A test mixture of eleven silicon model compounds was used in this work. Siloxanes (cyclic and linear), silanols and silanes were selected based on their identification in synthetic PDMS degradation samples¹⁶ and thus, on their possible presence in petroleum products:^{3,17} trimethylsilanol (*TMSOH*, b.p 98°C); pentamethyldisiloxane (*A*, b.p 80°C); hexamethyldisiloxane (*L2*, b.p 100°C); triethylsilane (*F*, b.p 107°C); hexamethylcyclotrisiloxane (*D3*, b.p 134°C); octamethyltrisiloxane (*L3*, b.p 153°C); octamethylcyclotetrasiloxane (*D4*, b.p 175°C); decamethyltetrasiloxane (*L4*, b.p 194°C); decamethylcyclopentasiloxane (*D5*, b.p 211°C); dodecamethylpentasiloxane (*L5*, b.p 210°C); dodecamethylcyclohexasiloxane (*D6*, b.p 245°C). Tetrakis(trimethylsilyloxy)silane (*M4Q*, b.p 106°C) was used as internal standard to consider density difference between heptane and real samples as well as potential sample evaporation during the analysis (more details in "Analytical figures of merit and method validation" section). Individual standards of silicon compounds were purchased from Sigma-Aldrich (L'Isle d'Abeau, France) and Interchim (Montluçon, France). A mixture of these silicon compounds was prepared in heptane (VWR, quality Normapur, Fontenay sous Bois, France). Different dilutions were prepared to calculate quantification limits and to build the calibration curves. Specific vials in polypropylene with septa caps only made of PTFE provided by VWR (Fontenay sous Bois, France) in replacement of classical septa made of silicones to avoid cyclic siloxane contaminations were used. More details on the complete analytical procedure for Si speciation were already reported in Chainet *et al.*^{11,15} to avoid potential contaminations and artifacts.

Samples. Two gasolines without silicon, one from direct distillation of crude oil (Straight-Run Gasoline) and the other from fluid catalytic cracking (FCC Gasoline) were used to evaluate matrix effects. One reforming naphtha (Naphtha), without silicon was analyzed as quality control (QC) after spiking it with model silicon compounds at around 250 μ g kg⁻¹. Three coker naphthas (coker naphthas A, B and C) originated from different refineries were also studied. Note that coking is a refining process based on thermal cracking at 500 °C of heavy petroleum products into lighter cuts

(diesel or naphtha). PDMS is generally used as antifoaming to minimize the generation of emulsions in this process. Table 1

View Article Online
DOI: 10.1039/DOJA00156B

Table 1. Physicochemical characteristics of the samples analyzed.

Properties	Methods	Gasolines			Coker naphthas		
		Straight-Run Gasoline	FCC Gasoline	Reforming Naphtha	A	B	C
Density (g cm ⁻³)	NF EN ISO 12185	0.7481	0.6820	0.7422	0.7735	0.7635	0.7241
Boiling range (°C)	IFPEN 9302	23-230	23-107	74-158	69-219	0-294	0-208
Sulphur concentration (mg kg ⁻¹)	NF ISO 20884	385	587	<0.3	12192	9810	5632
Nitrogen concentration (mg kg ⁻¹)	ASTM D4629	40.1	0.44	<0.3	133	206	103
RON [#]	IFPEN 9302	90.4	64	Nd	66	nd	67
n-Paraffins concentration (%wt)		48.9	39.10	27.39	19.92	nd	29.45
Isoparaffins concentration (%wt)			36.71	28.99	0.92	nd	1.90
Naphthens concentration (%wt)			19.98	30.48	8.65	nd	9.30
Aromatics concentration (%wt)		26.1	4.13	13.15	34.24	16.87*	28.4
Olefins concentration (%wt)		25	0.07	Absent	18.2	nd	12.6

nd: not determined; *Determined by UV method; [#] RON: research octane number

summarizes the samples provided by IFP Energies Nouvelle (Solaize, France) and their characteristics determined by standard methods for density, sulfur, and nitrogen concentration and by IFPEN 9302³³ internal method for boiling range and hydrocarbon composition.

Instrumentation

GC-ICP-MS/MS apparatus. All measurements were carried out using an Agilent 7890B GC (Agilent Technologies, USA) coupled to an Agilent 8800 ICP-QQQ instrument (Agilent Technologies, USA) using an Agilent GC-ICP-MS transfer line (Agilent Technologies, Japan). The GC-ICP-MS interface consists of a passivated transfer line (sulfinert) with an injector tube both heated at 300°C and a special torch. The GC column was connected *via* a T piece to a pre-heating pipe for supplying the argon carrier gas in order to sweep the GC column effluents through the transfer line into the plasma. In this way, the sample was maintained at a constant high temperature from the end of the chromatographic column in the GC oven to the tip of the ICP injector. Using the electronic pneumatic control (EPC) module, a mixture argon/oxygen (80/20) as optional gas (OG) was added to the Ar carrier gas to burn carbon deposits coming from the samples. A mixture of Xe at 0.1% in He (Air liquide, France) was used as an alternate GC carrier gas to tune the ICP-MS/MS (resolution and mass axis) for the maximum of sensitivity on the ¹²⁴Xe m/z value. Using the ICP-MS/MS for Si, Q1 and Q2 were set to m/z 28 because there was no reaction with H₂ in the cell.¹⁷ However, the main interferences of concern, ¹⁴N¹⁴N⁺ and ¹²C¹⁶O⁺ reacted with H₂ to form respectively ¹⁴N¹⁴N¹H⁺ and ¹²C¹⁶O¹H⁺ (m/z 29) and were minimized by Q2 set at 28. More details on the operating conditions of the GC-ICP-MS/MS system are listed in Table 2.

ICP-OES apparatus. An Optima 7300 DV Perkin-Elmer ICP-OES spectrometer (Uberlingen, Germany) was used to determine total Si at trace levels and the emission signals were axially taken. A concentric micronebulizer fitted to the high temperature Torch Integrated Sample Introduction System (hTISIS) was used as sample introduction system.¹² The hTISIS temperature was set at 400°C and the sample was aspirated at 30 μL min⁻¹ according to an air segmented injection regime.³⁴ The solutions were delivered to the nebulizer by means of a peristaltic pump (Perimax 16 antiplus, Spetec, Erding, Germany) and a 0.19-mm id flared end PVC-based tubing (Glass Expansion, Melbourne, Australia) was employed.

XRF apparatus. The total Silicon content was also determined following an internal IFPEN method.³⁵ A Panalytical Axios (Almelo, Netherlands) 4 kW equipped with a Cr anode was used to perform the wavelength dispersive X-rays fluorescence (WDXRF) analysis. A 2 mL minimum solution volume was introduced within a cup with a polypropylene 6 μm film. The quantification limit was 10 mg kg⁻¹ of Si with a measuring time of 30 seconds to avoid the evaporation of the light petroleum products.

Table 2. Operating conditions of the GC-ICP-MS/MS system.

GC Conditions	
Injection	1 μL in Split 1:10 mode at 280°C through a Merlin Microseal system
Carrier gas	He at 2 mL min ⁻¹
Column	DB-5 MS UI (30m x 0.25mm x 0.25 μm)
Oven program temperature	35°C (5min) → 140°C at 10°C min ⁻¹ → 250°C at 20°C min ⁻¹
Transfer line and Injector temperature	300°C

ICP-MS/MS detection conditions (*optimized conditions in italics*)

Cones Type	Pt cones	32
Sample depth	8 mm.	33
RF Power	1550 watts	34
Carrier gas flow (CG)	Ar at 0.4-0.8 L min ⁻¹ (0.5 L min ⁻¹)	35
Optional gas flow (OG)	Ar/O ₂ (80/20) at 0-0.25 L min ⁻¹ (0.15 L min ⁻¹)	36
ORC Gas flow	H ₂ at 0-3.0 mL min ⁻¹ (2 mL min ⁻¹)	37
Isotopes monitored	²⁸ Si → ²⁸ Si	38
Q1 → Q2	¹³ C → ¹³ C; ³⁷ ArH → ³⁷ ArH; ³⁸ Ar → ³⁸ Ar	39 40 41

Results and discussion

Optimization of the GC-ICP-MS/MS operating parameters

A 1 mg kg⁻¹ solution of octamethylcyclotetrasiloxane (D4) heptane was taken as a model because it (and D3) was the most recovered compound in synthetic PDMS degradation samples. Furthermore, its boiling point is close to those for real naphtha samples. Therefore, this compound was used both for the optimization of the carrier (CG), optional (OG) and hydrogen gas flow rates.

Optimization of the carrier gas and optional gas flow rates. As Figure 1 shows, the highest signal to noise ratio values were obtained for a CG equal to 0.5 L min⁻¹ and an OG of 0.15 L min⁻¹. For carrier gas flow rates higher than 0.6 L min⁻¹, the S/N ratio dropped and the reproducibility became poor. This could be explained by a degradation of the thermal characteristics of the plasma caused by the increase in the total gas plasma load.

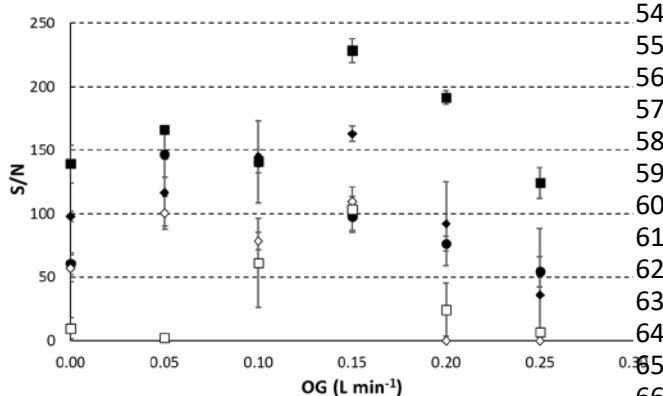


Figure 1. Signal-to-noise ratio (S/N) for D4 as a function of the carrier (CG) and optional (OG) gas flow rates. Carrier gas flow rates: 0.4 L min⁻¹ (black circles); 0.5 L min⁻¹ (black squares); 0.6 L min⁻¹ (black diamonds); 0.7 L min⁻¹ (white diamonds); 0.8 L min⁻¹ (white squares). H₂ gas flow rate: 0.5 mL min⁻¹. The values corresponded to the average ± standard deviation (3 replicates were measured).

Taking into account that the optional gas consisted of a mixture of Ar/O₂ (80/20), under optimum conditions (CG = 0.5 L min⁻¹; OG = 0.15 L min⁻¹) the oxygen gas flow rate represented 6% of the total gas introduced into the plasma. The amount of O₂ added under these conditions was enough for the complete conversion of C

CO, thus avoiding the carbon soot deposits in the cones. Plasma degradation could be evaluated by following the signal of the Ar isotope. Figure 2 shows the superimposition of the ²⁸Si chromatogram and the evolution of ³⁸Ar signal with time for two different situations: (i) the optimal values of carrier and optional gas flow rates in terms of S/N; and, (ii) values of carrier and optional gas flow rates equal to 0.4 L min⁻¹ and 0.1 L min⁻¹, respectively. For a given set of operating conditions, two peaks were found. A first one appearing at around 1.9 min that corresponded to heptane and a second one that was due to the elution of the D4 silicon compound at approximately 2.5 min. The former peak was found at a 28 m/z ratio (see dashed lines in Figure 2) since only 0.5 mL min⁻¹ of hydrogen were added to the cell (fixed value before the ORC optimization). Therefore, this peak revealed the magnitude of the interference of ¹²C¹⁶O⁺ that, as expected, was more intense for the optimum conditions than when the total gas flow (CG+OG) was lower. It should also be mentioned that when heptane arrived to the plasma, the ³⁸Ar signal decreased (Figure 2) by roughly a 20% and 75% for CG=0.4 L min⁻¹ and OG=0.1 L min⁻¹ and optimal conditions, respectively, that demonstrated the detrimental impact of the solvent on the plasma ionization characteristics. (Figure 2).

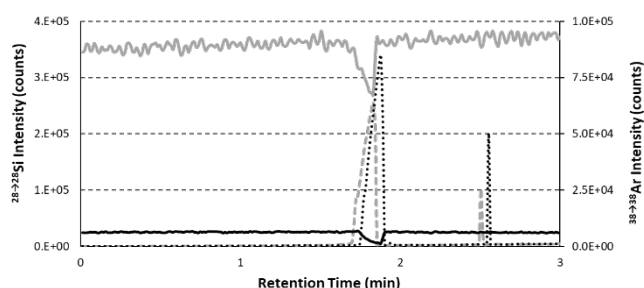


Figure 2. ²⁸Si (dashed lines) and ³⁸Ar (continuous lines) chromatogram for the D4 at 1 mg kg⁻¹ in heptane. Grey: carrier and optional gas flow rate: 0.4 L min⁻¹ and 0.10 L min⁻¹; black: 0.5 L min⁻¹ and 0.15 L min⁻¹. H₂ gas flow rate: 0.5 mL min⁻¹.

Optimization of the octopole reaction cell (ORC). When experiments were performed before the optimization of the ORC, the heptane peak at m/z 28 due to the ¹²C¹⁶O⁺ interference was observed (Figure 2). With the injection of up to 2 mL min⁻¹ of H₂, the ¹²C¹⁶O⁺ interference was minimized without any degradation in sensitivity. To illustrate the H₂ optimization, GC-ICP-MS/MS chromatograms are available in Figure S1. For example, a diminution of the heptane peak intensity by a factor of 30000 when switching from 0.5 to 2 mL min⁻¹ of H₂ was observed, whereas a diminution factor of 16 was found for D4 (Figure S1). As Figure 3 shows, for this silicon compound, the signal to noise ratio (S/N) was not drastically affected, because the standard deviation of the background noise decreased with the H₂ gas flow rate. The highest D4 signal to noise ratio was obtained for the 1.5 mL min⁻¹, however at this flow rate a ¹²C¹⁶O⁺ interference due to the heptane was still observed (Figure 3 and Figure S1). For that reason, 2.0 mL min⁻¹ of H₂ was selected as optimum value, as it represented a compromise between the S/N ratio and the minimization of the ¹²C¹⁶O⁺ interference. At flow rates higher than 2.0 mL min⁻¹, the S/N was

drastically reduced. In fact, at 3.0 mL min⁻¹ the D4 peak height decreased by a factor of 180 (Figure 1S).

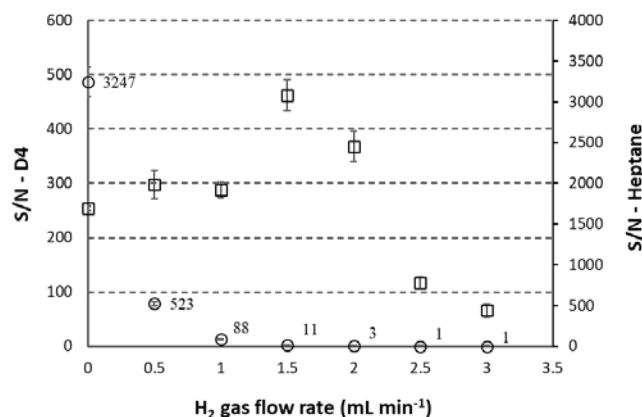


Figure 3. Signal-to-noise ratio (S/N) for D4 and heptane as a function of the hydrogen flow rate. Carrier gas flow rate: 0.5 L min⁻¹; optional gas flow rate: 0.15 L min⁻¹. The values corresponded to the average \pm standard deviation (3 replicates were measured). Circles: heptane; squares: D4.

Analytical performances and validation of GC-ICP-MS/MS method

Separation of silicon compounds in a spiked sample. A sample of FCC gasoline was spiked with the mixture containing 50 $\mu\text{g kg}^{-1}$ of the silicon model compounds and analyzed by GC-ICP-MS/MS under the optimized conditions. Figure 4 shows the evolution of ¹³C with time together with the chromatogram for ²⁸Si obtained for this sample. It can be verified that the matrix did not cause any distinguishable peak in the chromatogram obtained for silicon (see grey area in Figure 4). The signal recording for ¹³C corresponded to non-silicon containing organic compounds. As it may be observed there was a mismatching between the ²⁸Si peaks and those for carbon. The overcoming of the interference of ¹²C¹⁶O⁺ allowed to determine all the injected silicon compounds (even the most volatile ones such as TMSOH) at a concentration as low as 50 $\mu\text{g kg}^{-1}$ of Si.

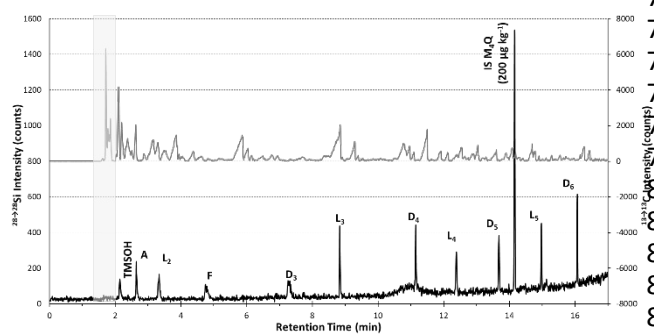


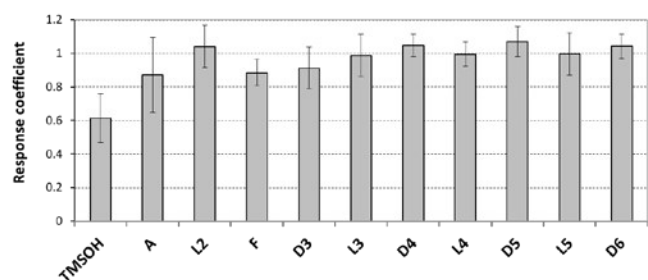
Figure 4. GC-ICP-MS/MS chromatograms of the 50 $\mu\text{g kg}^{-1}$ spiked FCC gasoline. Grey line: ¹³C; black line: ²⁸Si. Carrier gas flow rate: 0.5 L min⁻¹; optional gas flow rate: 0.15 L min⁻¹, H₂ gas flow rate: 2.0 mL min⁻¹.

Sample matrix and silicon chemical form effect. Calibration curves ranging from 0 to 500 $\mu\text{g kg}^{-1}$ were prepared with the eleven silicon compounds in three different matrices: heptane (two calibration curves were prepared in different days), and two gasolines without silicon-containing compounds (a straight-run gasoline and a FCC gasoline, with different physico-chemical characteristics (Table 1)). Calibration curves ($y = ax$) for each compound (C) were calculated, where y corresponded to $\frac{\text{Area C}}{\text{Area IS}}$ and x was the $\frac{\text{Concentration C}}{\text{Concentration IS}}$ ratio. IS refers to the internal standard M4Q added in both calibration samples at a precisely known concentration around 250 $\mu\text{g kg}^{-1}$ of silicon.

In order to evaluate the effect of the matrix on the analytical response, the slopes of the calibration curves were considered in relative terms. Thus, for each silicon model molecule, the slope obtained for the calibration curve prepared by using each gasoline and one of the replicates of the heptane was divided by that obtained for the second replicate of heptane. The relative slopes were close to unity regardless of the Si compound (Figure S2). The variation between the slopes was less than 10%, except for the most volatile compounds. In fact, the values of the slopes obtained for TMSOH were 15-20% higher when the FCC gasoline and heptane samples were analyzed than in the case of the straight-run gasoline (Figure S2). Meanwhile, the slope ratio in the case of compound A also deviated significantly from the unity when analyzing the straight-run gasoline. This could be explained by the evaporation of the silicon compounds over the time, as the second replicate for heptane was taken as reference. In any case, globally speaking, these results revealed that under the optimal conditions, matrix effects were mitigated (Figure S2).

Contrarily to what Chainet *et al.*¹⁷ and Grümping *et al.*³⁶ observed, in the present work, a virtually universal response was found for all silicon compounds (Figure 5). One of the hypotheses to explain the non-universal response in previous reports was the addition of cold argon (22 °C) at the exit of the GC column, thus causing a cold point in the transfer line and a potential decrease in the transfer efficiency to the ICP-MS for some silicon species.¹⁷ To overcome this problem, the temperature of the transfer line was set to 300°C and the cold argon was pre-heated in the oven of the GC before injection. As Sánchez *et al.*^{12,37} demonstrated using a total sample consumption system heated at 350°C, the so-called hTISIS allowed to minimize the effect of the silicon chemical form and the matrix on the ICP-signal. In the present work, the average and the confidence interval (as 3 x standard deviation) of the slope obtained in the different matrices and different days for each silicon compound were calculated. Thus, the slope corresponded to the response coefficient of each silicon compound and was equal by definition to the unity for the IS. As Figure 5 shows, the GC-ICP-MS/MS response was similar irrespectively of the silicon chemical form, except for the most volatile compound, trimethylsilanol (TMSOH) and pentamethyldisiloxane (A). The confidence interval is around 20% for these volatile compounds but less than 13% for the others. Similarly to the findings in the Chainet *et al.* work,¹⁷ TMSOH presented a lower response. As the calibration curve for TMSOH was linear ($R^2=0.9965$), the lower response observed was probably due to the evaporation of this compound regarding its volatility. This hypothesis was evaluated by the introduction of quality control

1 samples (QC) over the analytical run. The QC samples were
 2 prepared by spiking the reforming naphtha (Table 1) at 250 $\mu\text{g kg}^{-1}$
 3 level with the Si test mixture. As Figure S3 shows, recovery for the
 4 most volatile compounds, especially for TMSOH, decreased over the
 5 time. This parameter went from approximately 112 to 60%, thus
 6 proving the evaporation from the vial of this compound. Similar
 7 behavior was found for the compound A, but in this case the
 8 recovery values decreased by a factor of 20% over the time (Figure
 9 S3). Therefore, the influence of the silicon chemical form on the
 10 sensitivity was not caused by an instrumental bias.



11 **Figure 5.** Response coefficients for each silicon compound obtained
 12 using GC-ICP-MS/MS related to IS. Carrier gas flow rate: 0.5 L min⁻¹,
 13 optional gas flow rate: 0.15 L min⁻¹, H₂ gas flow rate: 2.0 mL min⁻¹.
 14 The value was represented as average \pm confidence interval (four
 15 calibration curves were measured).

16 **Analytical figures of merit and method validation.** One of the
 17 challenges to achieve a good peak definition and, thus, repeatability
 18 in GC-ICP-MS/MS is the need for a compromise between the
 19 number of points per peak and the signal to noise ratio.
 20 Repeatability of the method was evaluated by obtaining three
 21 replicates of the chromatograms for a 1 mg kg⁻¹ solution of
 22 prepared in heptane at different dwell times. At the highest value
 23 of dwell time the peak was poorly defined, thus degrading the
 24 repeatability of the method. The relative standard deviation of the
 25 peak area was approximately 10%. The highest signal to noise ratio
 26 was obtained for a dwell time equal to 0.2 s. However, the
 27 maximum number of points per peak and the lowest relative
 28 standard deviation of the peak area values were obtained at 0.1 s
 29 dwell time. Therefore, the latter value was taken as the optimum
 30 one.

31 One of the most relevant analytical figures of merit is the limit
 32 of quantification (LOQ). The determinations of the limit of detection
 33 (LOD) and LOQ are based on the calculation of 3 and 10 times the

34 absolute standard deviation of the background, respectively. In
 35 the present work, the minimum concentration that can be
 36 accurately measured by GC-ICP-MS/MS according to the described
 37 quantification method was determined. Spiked heptane and
 38 gasoline solutions, considered now as samples, were analyzed using
 39 a heptane calibration curve prepared in a different day. An
 40 acceptable confidence interval of 20% between the known and the
 41 experimentally determined concentration was chosen to validate
 42 the LOQ. The results revealed that this parameter ranged from 8 to
 43 60 $\mu\text{g kg}^{-1}$, except for the three most volatile compounds (TMSOH, A
 44 and L2) in heptane (Table 3). The obtained LOQ in the case of L2 in
 45 heptane was likely due to its peak shape distortion induced by the
 46 high amount of heptane leaving the GC capillary phase at the same
 47 retention time. This chromatographic issue was not observed in
 48 gasolines. Quantification limits were compared with the previous
 49 values obtained by Chainet *et al.*¹⁷ Under optimized conditions, the
 50 GC-ICP-MS/MS method presented lower LOQ values than those
 51 obtained in the previous work. The improvement factor ranged
 52 from 2 to 28, depending on the silicon compound.

53 The linearity of the GC-ICP-MS/MS was studied for a
 54 concentration range from 0 to 500 $\mu\text{g kg}^{-1}$ of silicon in heptane. The
 55 ICP-MS/MS response was linear with correlation coefficients up to
 56 0.999. Method applicability was tested by measuring six quality
 57 control standards (QC) distributed throughout the analytical run to
 58 assess a possible drift in the analytical signals. They were prepared
 59 by spiking one reforming naphtha (Table 1) at 250 $\mu\text{g kg}^{-1}$ level with
 60 a Si test mixture. For the family of cyclic siloxanes (D3, D4, D5 and
 61 D6), calculated recovery values ranged from 92-109%; whereas for
 62 the remaining silicon compounds the recoveries were in the 80-
 63 120% range, except for TMSOH. In this case, recovery decreased
 64 over the analytical run (Figure S3). This behavior could be explained
 65 by TMSOH evaporation from the vial with time. Note that TMSOH
 66 was the most volatile silicon compound. Regression analysis³⁹ of QC
 67 data were performed and no systematic trends at 95% of
 68 confidence level were visible, except for trimethylsilanol (TMSOH).
 69 These results clearly validated the GC-ICP-MS/MS method for the Si
 70 speciation in light petroleum products and could be applied to real
 71 coker naphtha samples.

72 Analysis of real coker naphtha samples

73 For speciation analysis, coker naphthas were diluted in heptane to
 74 fit the calibration curve range from 0 to 500 $\mu\text{g kg}^{-1}$. The GC-ICP-

75 **Table 3.** Limit of quantification (LOQ) ($\mu\text{g kg}^{-1}$) and retention time (min) obtained for each silicon compound.

Silicon compound	Retention time (min)				
	Heptane	Straight-run Gasoline	FCC Gasoline	Acetone Chainet ¹⁷	
TMSOH	80	44	24	57	
A	77	43	18	nc	
L2	177	8	8	77	
F	8	8	8	227	
D3	49	25	25	85	
L3	12	31	55	112	
D4	49	49	49	112	
L4	44	10	44	110	
D5	47	47	47	83	
L5	24	24	24	78	

D6	16.02	33	58	58	63
nc: not considered					DOI: 10.1039/DOJA00156B

Table 4. Silicon species and total Si concentration (mg kg^{-1}) obtained by GC-ICP-MS/MS^a, ICP-OES^a and XRF^b.

Coker Naphtha	Dilution factor	D3	D4	D5	D6	Total GC-ICP-MS/MS	Total hTISIS-ICP-OES	Total XRF
A	70	9.0 ± 0.3	6.0 ± 0.4	2.7 ± 0.4	1.27 ± 0.10	20.0 ± 1.3	19.9 ± 1.4	19 ± 10
B	20	0.89 ± 0.14	0.36 ± 0.10	nd	nd	1.3 ± 0.2	1.55 ± 0.14	<10
C	80	5.2 ± 0.2	2.5 ± 0.9	nd	nd	8.0 ± 0.7	7.6 ± 0.6	<10

nd: not detected; ^aThe values corresponded to the average $\pm 3 \times$ standard deviation (3 replicates); ^bThe values were the average \pm method confident interval (2 replicates)

MS/MS chromatogram obtained for the coker naphtha A is illustrated in Figure 6. Four cyclic siloxanes D3-D6 were identified according to their retention times (Table 3) and quantified on the sample. One unknown silicon peak, likely coming from the column bleeding was also present at around 15 minutes. This peak was also detected in blanks and QC but it did not overlap with the analytes. GC-ICP-MS/MS chromatograms of coker naphthas B and C are also illustrated in Figure S4. No other silicon compound was detected in the three coker naphthas. These results confirmed that cyclic siloxanes (Dn) were the main PDMS thermal degradation products in synthetic PDMS degradation samples¹⁷ and real naphthas,³ oil and gas process conditions could clearly influence the formation of other silicon compounds but at very low level compared to cyclic siloxanes.

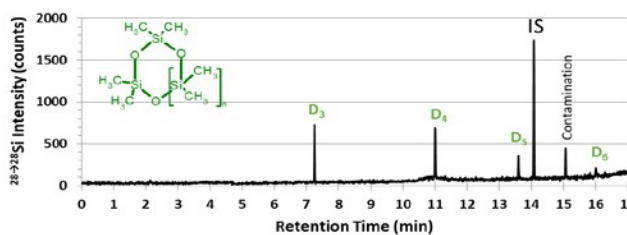


Figure 6. GC-ICP-MS chromatogram of the coker naphtha A sample (IS: internal standard). Carrier gas flow rate: 0.5 L min^{-1} ; optional gas flow rate: 0.15 L min^{-1} , H_2 gas flow rate: 2.0 mL min^{-1} .

To validate the speciation method by GC-ICP-MS/MS, we must verify that all silicon species are identified and quantified. As no certified reference materials exist for Si speciation in petroleum products, the sum of the concentrations of Si species was compared to the total Si content. Total silicon concentration was determined by XRF and ICP-OES, especially for low Si concentration, and then compared to the GC-ICP-MS/MS results for the validation of the method. Table 4 reveals that there were no differences between the total Si concentration in coker naphtha A for the three employed methods (coefficient of variation less than 3%). The coefficient of variation between the GC-ICP-MS/MS and ICP-OES results for coker naphthas B and C, with total Si content below the XRF LOQ, were respectively lower than 12% and 4%. These results demonstrated that all silicon species were properly identified and quantified. Therefore, the developed GC-ICP-MS/MS was validated for silicon speciation in petroleum samples.

Conclusions

The main goal of this work was to develop a method for silicon speciation in light petroleum products based on GC-ICP-MS/MS. The main concern of ²⁸Si determination by ICP-MS related with the spectral interferences due to the formation of ¹²C¹⁶O⁺ and ¹⁴N¹⁴N⁺ has been eliminated by adding hydrogen as reactant gas in the octopole reaction cell (ORC). The optimization of the GC-ICP-MS/MS operating parameters (carrier gas, optional gas and hydrogen gas flow rates) plays a crucial role to obtain a detector response independently of sample matrix and silicon chemical form. Moreover, LOQ values ranged from 8 to $60 \mu\text{g kg}^{-1}$.

GC-ICP-MS/MS method has been validated by the analysis of different petroleum derivatives. Cyclic siloxanes (D3-D6) were confirmed as the main silicon compounds present in coker naphtha samples. The proposed GC-ICP-MS/MS and two alternative analytical methods (ICP-OES and XRF) have provided similar total Si concentrations and have demonstrated that all silicon species have been taken into account. Therefore, the new method could be applied to the determination of Si catalyst contaminants in light petroleum products. The achievement of silicon speciation in real coker naphthas will allow the development of trapping systems to remove these compounds before hydrotreatment catalysts.

Conflicts of interest

There are no conflicts to declare.

Acknowledgements

The authors wish to thank the Spanish Ministry of Science, Innovation and Universities for the financial support (Project Ref. PGC2018-100711-B-I00), and L. Ayouni and F. Bessueille (Université de Lyon, Institut des Sciences Analytiques, UMR 5280, CNRS, Université Lyon 1, ENS Lyon - 5, rue de la Doua, F-69100 Villeurbanne, France) for all their advices on ICP-MS/MS, which have helped to achieve this work. Special acknowledgments go to Agilent (France) and especially to B. El Moujahid and G. Alloncle during GC-ICP-MS transfer line installation and for their technical assistance, and S. Sannac for all its advices.

References

Journal Name

ARTICLE

- 1 F. Chainet, C.P. Lienemann, M. Courtiade, J. Ponthus and O.F.X. Donard, *J. Anal. At. Spectrom.*, 2011, **26**, 30-51. 42
- 2 Donard, *J. Anal. At. Spectrom.*, 2011, **26**, 30-51. 43
- 3 P. Dufresne, *Appl. Catal. A*, 2007, **322**, 67-75. 44
- 4 A.C. Dubreuil, F. Chainet, R.M. de Sousa Bartolomeu, F.M. Mota, J. Janvier and C.P. Lienemann, *C.R. Chimie*, 2017, **20**, 66. 45
- 5 66. 47
- 6 R.G. Nuzzo, L.H. Dubois, N.E. Bowles and M.A. Trecoske, *Catal.*, 1984, **85**, 267-271. 48
- 7 A. Molnar, I. Bucsi, M. Bartok, F. Notheisz and G.V. Smith, *J.Catal.*, 1986, **98**, 386-391. 49
- 8 G.V. Smith, S. Tjandra, M. Musoiu, T. Wiltowski, F. Notheisz, Bartok, I. Hannus, D. Ostgard and V. Malhotra, *J. Catal.*, 1995, **161**, 441-450. 50
- 9 R. Breivik and R. Egebjerg, *Petrol. Tech. Q.*, 2008, **1**, 69-74. 51
- 10 C. Rome and T.G. Hueston, *Silicone in the Oil and Gas Industry*, Dow Corning Corporation, 2002. 52
- 11 T. Tran, P. Griпка and L. Kraus, *Petrol. Tech. Q. Catalysis*, 2018, 31-33. 53
- 12 G. Camino, S.M. Lomakin and M. Lagueard, *Polymer*, 2002, 2011-2015. 54
- 13 F. Chainet, M. Courtiade, C.P. Lienemann, J. Ponthus and O.F.X. Donard, *J. Chromatogr. A.*, 2011, **1218**, 9269-9278. 55
- 14 R. Sánchez, J. L. Todolí, C.P. Lienemann and J. M. Mermet, *Anal. At. Spectrom.*, 2012, **27**, 937-945. 56
- 15 M.F. Gazulla, M. Rodrigo, M. Orduña, M.J. Ventura and Andreu, *Talanta*, 2017, **164**, 563-569. 57
- 16 P. Pohl, N. Vorapalawut, B. Bouyssiere and R. Lobinski, *J. Anal. At. Spectrom.*, 2010, **25**, 1461-1466. 58
- 17 F. Chainet, J. Ponthus, C.P. Lienemann, M. Courtiade and O.F.X. Donard, *Anal. Chem.*, 2012, **84**, 3998-4005. 59
- 18 F. Chainet, L. Le Meur, M. Courtiade, C.P. Lienemann, J. Ponthus and O.F.X. Donard, *Fuel*, 2014, **116**, 478-489. 60
- 19 F. Chainet, C.P. Lienemann, J. Ponthus, C. Pecheyran, J. Castro E. Tessier and O.F.X. Donard, *Spectrochim. Acta B*, 2014, **97**, 56. 61
- 20 F. Chainet, L. Le Meur, M. Courtiade, C.P. Lienemann, J. Ponthus, L. Brunet-Errard and O.F.X. Donard, *Fuel Process Technol.*, 2012, **104**, 300-309. 62
- 21 C.H. Yang and S.J. Jiang, *Spectrochim. Acta B*, 2004, **59**, 1388-1394. 63
- 22 N. Jakubowski, L. Moens and F. Vanhaecke, *Spectrochim. Acta B*, 1998, **53**, 1739-1763. DOI: 10.1039/DOJA00156B
- 23 P. Pohl, J. Dural, N. Vorapalawut, I. Merdrignac, C.P. Lienemann, H. Carrier, B. Grassl, B. Bouyssiere and R. Lobinski, *J. Anal. At. Spectrom.*, 2010, **25**, 1974-1977.
- 24 S.D. Tanner, V.I. Baranov and D.R. Bandura, *Spectrochim. Acta B*, 2002, **57**, 1361-1452.
- 25 P.L. Dupont, C. Galvez, N. Le Grand and P. Kaluzny, *Spectr. Anal.*, 2009, **267**, 44-50.
- 26 H.T. Liu and S.J. Jiang, *Spectrochim. Acta B*, 2003, **58**, 153-157.
- 27 M. Ben-Younes, D.C. Gregoire and C.L. Chakrabarti, *Spectrochim. Acta B*, 2003, **58**, 361-372.
- 28 R.S. Amais, C.D.B. Amaral, L.L. Fialho, D. Schiavo and J.A. Nóbrega, *Anal. Methods*, 2014, **6**, 4516-4520.
- 29 D. Foppiano, M. Tarik, J. Schneebeli, A. Calbry-Muzyka, S. Biollaz and C. Ludwig, *Talanta*, 2020, **208**, 120398.
- 30 E. Bolea, L. Balcaen, M. Resano and F. Vanhaecke, *J. Anal. At. Spectrom.*, 2017, **32**, 1660-1679.
- 31 F. Chainet, A. Desprez, S. Carbonneaux, L. Ayouni, M.L. Milliand and C.P. Lienemann, *Fuel Process. Technol.*, 2019, **188**, 60-69.
- 32 J. Nelson, H. Hopfer, F. Silva, S. Wilbur, J. Chen, K. Shiota Ozawa and P. L. Wylie, *J. Agric. Food Chem.*, 2015, **63**, 4478-4483.
- 33 L. Freije-Carrelo, J. García-Bellido, F. Calderón-Celis, M. Moldovan and J. R. Encinar, *Anal. Chem.*, 2019, **91**, 7019-7024.
- 34 G. Radermacher, H. Rüdell, C. Wesch, A. Böhnhardt and J. Koschorreck, *Sci Total Environ*, 2020, **706**, 136011-136017.
- 35 Detailed analysis by gas chromatography for gasoline, *IFPEN 9302 Internal method*, 2015.
- 36 C. Sánchez, C.P. Lienemann and J.L. Todolí, *Spectrochim. Acta, Part B*, 2016, **124**, 99-108.
- 37 Silicon determination in gasoline by XRF, *IFPEN Internal method*, 2016.
- 38 R. Grümping, D. Mikolajczak and A.V. Hirner, *Fresenius J. Anal. Chem.*, 1998, **361**, 133-139.
- 39 R. Sanchez, J.L. Todoli, C.P. Lienemann and J.M. Mermet, *J. Anal. At. Spectrom.*, 2009, **24**, 1382-1388.
- 40 V. Thomsen, D. Schatzlein and D. Mercurio, *Spectroscopy*, 2003, **18**, 112-114.
- 41 *EURACHEM Guide: The fitness for purpose of analytical methods: A laboratory guide to method validation and related topics*; LGC Teddington, 1998.